Irregular bone defect repair via tissue-engineered periosteum approach in rabbit model.

Lin Zhao
Shanghai University and Health Sciences affiliated Zhoupu Hospital
Jia-Jia Yu
Department of Joint Sugery of Yuncheng Central Hospital of Shanxi Province
Cangyu Zhang
Orthopedic Department of the 2nd Hospital of Lanzhu University
Xiuhui Wang (xiuhuiwang007@126.com)
Shanghai University of Medicine and Health Sciences affiliated Zhoupu Hospital

Research article

Keywords: Tissue engineering, Periosteum, Irregular bone, Bone defect

Posted Date: December 19th, 2019

DOI: https://doi.org/10.21203/rs.2.19343/v1

Abstract

Background

As an alternative of bone grafts for defect repair, tissue engineering is much promising for clinical application. In previous studies, we have succeeded in repair of long bone defect with homemade tissue-engineered periosteum (TEP), of which is fabraicated by incorporating osteogenically induced mesenchymal stem cells (MSCs) of rabbits with a scaffold of small intestinal submucosa (SIS).

Methods

In this study, we are aimed to discuss the feasibility of allogenic irregular bone defect repair with the TEP. Thirty-six rabbits whose scapulas were subtotally resected to establish large irregular bone defects model in allogenic rabbits. The defects were treat respectively with TEP (Group 1, n=12), allogenic deproteinized bone (DPB) (Group 2, n=12) and hybrid of TEP and DPB (Group 3, n=12). At 4, 8, and 12 weeks after surgery, the rabbits were sacrificed, and the implants were harvested. X-ray radiographic and histological examinations were performed.

Results

The findings suggested that the radiographic score in TEP-DPB hybrided implantation (Group 3) was higher than TEP or DPB grafting only ($p<0.05$).But that was inconsistent with histological findings, which Group1 appeared to possess significantly higher bone formation than Group 2 ($p<0.05$) and Group3 has higher new bone volume than that of Group 2 ($p<0.05$).

Conclusion

We conclude that TEP is a promising alternative in repair of large irregular bone defect.DPB served as a 3D scaffold in combining TEP could provide mechanical support and shaping guide, but hinder new bone formation via TEP approach due to retard degradation.

Background

Massive bone defect remains a challenge for orthopedic surgeons [1–3]. Bone tissue engineering (BTE) is promising for bone defect reapair. Classical BTE approach is to select a biomaterial scaffold that provides structural support for 3D bone tissue formation [4, 5]. The limited bone tissue regeneration is mainly due to insufficient nutrient, oxygen delivery and metabolic waste removal within the 3D scaffolds [6]. Seeding cells on the outer surfaces of the 3D scaffolds may have sufficient nutrient, while cells located inside the scaffolds would be subjected to necrosis, which hinders the bone regeneration [7, 8]. In addition, in the absence of capillary network within the 3D implants, the engineered tissues can only have a maximum thickness of 150–200 mm; dimensions larger than this threshold may result in lack of oxygen inside the biomaterials [9, 10]. So many formidable conceptual and technical challenges impede clinical translation of experimental successes into clinical practices [5]. In the clinics, bone defects are

always in any size and any shape due to surgical treatment of tumors and other bone disease. Traditional treatment was not likely to repair them in original size and shape. Therefore, intensive efforts should be made to seek alternative approach.

The periosteum plays an indispensable role in both bone formation and bone defect healing via endogenous repair approach [11–13]. There are some papers have illustrated an approach using mesenchymal stem cell (MSCs) sheets or periosteal for bone healing [14–16]. There would be a great promise for fabrication of a biomimetic periosteum substitute that could fit any size and shape for bone defect repair [14].

Based on tissue-engineering principles, in previous studies, we have developed a flexible cellular construct that serves as an osteogenic and angiogenic “periosteum”, a kinde of homemade tissue-engineered periosteum (TEP),of which was fabraicated by incorporating osteogenically induced MSCs of rabbits with a scaffold of small intestinal submucosa (SIS). It has successfully reconstructed long bone critical size defect (CSD) in our previous studies [17, 18]. In this study, we hypothesize that TEP may repair large irregular bone defect in rabbit model.

Methods

Animals

46 New Zealand white rabbits (NZWRs), including of 36 adults (2months, about 2.0 kg) and 10 neonatals (2 weeks, about 0.40 kg), were invovled in this study. All the experimental procedures involving animals were approved by the Institutional Animal Care and Use Committee of Lanzhou University, China.

Cell culture and osteogenic induction

Cell culture and osteogenic induction were performed as previous studies [17, 18]. Briefly, bone marrow (5 mL) was aspirated from the ventral ilium of neonatal NZWRs (2 weeks, about 0.40 kg). Marrow mesenchymal stem cells (MSCs) isolated from bone marrow were collected and then planted in a plastic culture flask with Dulbecco’s modified Eagle medium (DMEM, Invitrogen, USA) containing 10% fetal bovine serum (FBS, Sijiqing, China) incubating at 37 ^{0}C with 5% CO_2. The primary passage MSCs were observed under microscopy and further confirmed with Giemsa staining .When MSCs reached 80–90% confluence, they were detached with 0.25% trypsin (Gibco, USA) and transferred to new culture flasks at a density of $2 \times 10^{6} L^{-1}$ and subcultured 2 times when the confluence reached 90%. The passage 3 MSCs were used for osteogenic differentiation with a standard DMEM supplemented with 50 mg L^{-1} ascorbic acid (Sigma, USA), 10 mmol L − 1 sodium β-glycerophosphate (Sigma, USA) and 10^{-8} mol L^{-1} dexamethasone (Sigma, USA) at 37 ^{0}C in a humidified 5% CO_2 incubator for 3 weeks. Successfully osteogenic induction was determined by formation of calcified colliculus from induced MSCs, by which can be inspected alizarin red staining. The osteogenically induced MSCs were collected as seeding cells.

TEP fabrication

The porcine small intestinal was cut in length of approximately 10 cm each, which was collected from healthy porcine (Lanzhou slaughter factory, Gansu Province) within 4 hours since sacrifice. Submucosa was obtained by mechanical removal of the tunica serosa and muscularis. Then the remaining submucosa layer was treated with a series of chemical decellularization, detergent treatment, lyophilization and sterilization [19]. Finally, all the samples were frozen-dried under − 70 ^{0}C with a lyophilizer, sealed into hermetic packages, and then sterilized by using Co-60 gamma irradiation (25–35 kGy).

The SIS was clipped into square (5 cm x 5 cm) and sterilized again under ultraviolet for 2 hours, then were soaked in DMEM containing 20% FBS for 1 day before cells seeding. The osteoblasts (osteoinduced for 2–3 weeks, 2.0×10^{9} L^{-1}) was slowly dripped onto SIS and incubated for 3 hourss at 37 ^{0}C. Then an appropriate volume of DMEM with 10% FBS was added to each composites, the incubation period lasted for 7 days.

Scanning electron microscopy (SEM)

Some of the tissue-engineered periosteum (TEP), which was cultured for 15 days, was collected for scanning electronmicroscopy (SEM JSW-680LA, Japan) inspection. Briefly, they were fixed in 2.5% glutaraldehyde for 7 days at room temperature, followed by washing thrice in PBS for 15 min each. After that, the specimens were subjected to critical point drying, gold sputter coating and then reviewed under SEM.

Preparation of deproteinized bone (DPB)

Fresh NZWR's scapular body harvested from surgical procedure of subtotal scapulectomy, which would be described below in detail, were deproteined in whole bone blocks after soft tissue removed. Densely vertical holes (each hole was 1.5 mm in diameter) were drilled into each block to make well deproteinization. The bone blocks were treated sequently with H_2O_2, NaN_3, NaOH, protease, methanol/chloroform mixture, ether, ethanediamine and absolute alcohol to produce DPB [20]. The samples were dried under 50 ^{0}C with dry oven, sealed into hermetic packages, and then sterilized by using Co-60 gamma irradiation (25–35 kGy).

Animal surgery and treatment

In strict accordance with the regulations of medical animal experiments, 36 NZWRs (2 months, about 2.0 kg) were anesthetized intraperitoneally with an injection of 3% pentobarbital solution (40 mg/kg, body weight). The unilateral shoulder of the rabbits was skinned and disinfected.The scapular body with

periosteum attached on it was exposed by buntly separating of the muscles, and resected off except for the glenoid and part of the scapular neck, angulus superior and inferior to establish a subtotal scapulectomy model. This model is aimed to preserve glenohumeral joint function for animal movement and prepare triangle anchoring points for implants attachment. Bone block from resection was removed together with the periosteum attached on it. The segmentally irregular bone defect was then created at unilateral shoulder blade of animal.

36 rabbits /defects were divided randomly into 3 groups with different treatment. The scapula defects were treated respectively with TEP (Group 1, n = 12), allogenic DPB (Group 2, n = 12), and TEP hybrid DPB (Group 3, n = 12).

In Group 1, TEP was spreaded over the defect area and trimmed the margins to fit the size and shape of the bone defect, then sutured with 7–0 microsurgical suture respectively to three bony anchoring points (mentioned above in bone resection part), which was pre-drilled several holes with K-wire for sutrure passing through. In Group 2, allogenic DPB block was fixed with steel wire (0.5 mm in diameter) respectively to three bony anchoring points. In Group 3, TEP enveloped DPB. Briefly, TEP wrapped on the surface of DPB and fixed with 7–0 microsurgical suture through vertical holes in DPB by a puerperal suture manner. Then the hybrid implants (TEP covered DPB) was fixed with steel wire (0.5 mm in diameter) respectively to three bony anchoring points. After implants were fixed tightly to the bony anchoring points with tension suture or K-wire, the incision was closed layer by layer with 1–0 nylon suture. The rabbits received 400,000 units penicillin preoperatively and at the first/next postoperative day. The forelimbs and shoulders of animals at surgical sides were immobilized with plaster casts for 4 weeks. The surgical procedure described is depicted using a schematic drawing, as seen in Fig. 1.

At 4, 8, and 12 weeks after surgery, four rabbits in each group were sacrificed under anesthesia and the whole scapula involved of implants were harvested as samples.

Radiographical evaluation

Radiological analysis of was performed at 4, 8 and 12 weeks postoperatively (DR3000 Dryview8900, Koda, Japan). The anteroposterior view of the scapula was obtained by X-ray. All radiographic results were evaluated in randomized and double-blind conditions. The Lane-Sandhu scoring system was applied for radiographic outcomes [21]. A defect was considered healed if the area of the newly formed bone exceeded 25% of the defect area according to bone healing critera of literature [9]. Radiographic scores were compared between the three groups.

Histological evaluation

Middle area tissue in experimental sites of scapula was excised out as specimens after X-ray radiographic examination. The specimens were fixed with 4% neutral-buffered for 3 days and decalcified

with10% EDTA-2Na solution for 4 weeks at 4°C. Then they were dehydrated with an ascending series of ethanol solutions, followed by serial paraffin sections by conventional method. Specimens were stained with hematoxylin & eosin (HE) and Masson for histological analysis.

All sections from each specimen were evaluated by light microscopy. Image analysis software (Pro-image Analysis System) was used to evaluate all sections per specimen. A region of interest (ROI) for quantitative evaluation of new bone formation was defined as the area of the tissue within the defect. The results were analyzed according to a histological numerical scoring system [22].

Statistical Analysis

Statistical analysis was performed with SPSS 15.0 software. All quantitative data were expressed as the mean ± standard deviation (M ± SD). Statistical comparison was performed by one-way analysis of variance (ANOVA) test. Statistical significance was considered at a probability < 0.05.

Results

Cell, scaffold and SEM

Under the light microscope, the MSCs showed a polygonal appearance at 3 day as well as uniform fibroblast-like appearance at passages 2 after induced for 2 weeks (Fig. 2a). HE staining can show nucleus and cytoplasm well (Fig. 2b).The induced MSCs showed the formation of calcified colliculus, by which can confirmed alizarin red staining (Fig. 2c).

Under macroscope, the homemade SIS scaffold was a white and flexible membrane with a 100 ± 20 μm thickness (Fig. 2d).The DPB imlpants were scalene triangle in shape with 5 ± 2 mm thickness and multiple holes in them (Fig. 2e). The TEP implants preserved the flexible nature and showed a membranous structure in gross view in culture dish (Fig. 2f). HE staining showed multiple cells on TEP (Fig. 2g).Under SEM, SIS was consisted of interlaced collagen fibers (Fig. 2h), while TEP has plenty of cells attached on SIS (Fig. 2i).

Physical examination of animals

The animals rapidly recovered within 1 hour after surgery and could stand well in 24 hours. All wounds closed within 1 week without any distinguished incision inflammation. In approximately 2 weeks, they were able to move freely. All animals remained in normal health throughout the course of the experiment.There was no evidence of infection or other complications in any animal.

Radiographical evaluation

The progress of bone defect repair was analyzed by radiography with a parallel comparison between the 1, 2 and 3 groups.

In Group 1, low-density calluses were observed at bone defect area at 4 weeks postoperation (Fig. 3a). At 8 weeks, more calluses were observed (Fig. 3b), and radiographic score was significantly higher than that of 4 weeks ($p < 0.05$). At 12 weeks, the newly formed bone volume and bone mineral density was highly increased (Fig. 3c), and radiographic score was significantly higher than that of 4 and 8 weeks ($p < 0.05$) (Fig. 4). Bony-union was achieved according to bone healing critera of literature [9].

In Group 2, there was very few DPB absorption and few callus formation observed at 4 weeks postoperation (Fig. 3d). At 8 weeks, DPB absorption was observed with few callus appeared at bone defect area (Fig. 3e). While the radiographic scores were no signifcant difference between 4 and 8 weeks. The radiographic score was no more than that of 4 weeks (p□0.05). At 12 weeks, DPB were absorbed further with some new bone formation (Fig. 3f). The radiographic score at this stage was significantly higher than that of 4 and 8 weeks ($p < 0.05$) (Fig. 4).

In Group 3, the holes on the DPB could not see clearly due to callus grew in them at 4 weeks (Fig. 3g). At 8 weeks, there was much more newly formed bone at bone defect area.The DPB was partially degraded and new bone formation was observed under X ray inspection (Fig. 3h). The bone mineral density was highly increased (Fig. 3i), and radiographic score was significantly higher than that of 4 and 8 weeks ($p < 0.05$) (Fig. 4). At 12 weeks postoperation, newly formed bone was substituted for degraded grafts, the radiopacity and appearance were close to that of the normal bone (Fig. 3i).

The findings suggested that the volume and bone mineral density of newly formed bone in Group 3 was significantly higher than that in Group 1 and Group 2, while Group1 was significantly higher than that of Group 2.

Histological evaluation

The speciments excised out from the scapular area were very similar to each other under the macroscope, and formed the approximate shape of scapula at 12 weeks (Fig. 3j, 3 k and 3 l).

Under the microscope, there was modest monocytes infiltration at 4 weeks in each group in HE staining.

In Group 1, there was newly formed immature osseous tissue and irregular vessels in the midst of degraded residuals of SIS and fibrous connective tissue. At 8 weeks, new osseous tissue was partially formed woven bone and mature vessels, while TEP almost degraded with few fibrous remnants and much scar tissue. At 12 weeks, all newly formed bone developed into mature cancellous bone under HE and Masson staining inspection (Fig. 5a ~ f).

In Group 2, DPB was degraded gradually at 4, and 8 weeks accompanied with few new osseous tissue formation. The new bone tissue formation was significantly abundant at 12 weeks than that of 4 and 8

weeks ($p < 0.05$). But the bone defect area was predominantly occupied by DPB even at 12 weeks (Fig. 5g ~ l).

In Group 3, there were amounts of newly osseous tissue formation accomanied with SIS and DPB degradation at 4 weeks. New osseous tissue formed woven bone at 8 weeks, while it was inclinded to form mature lamellar bone with osteoblasts embeded into mineral matrix at 12 weeks. The remnants of DPB were still abundant in defect area even at 12 weeks (Fig. 5m ~ r).

In comparison, Group 1 appeared to possess higher bone formation than Group 2 and 3 at 4, 8 and 12 weeks ($p < 0.05$ at 4 weeks, $p < 0.001$ at 8 and 12 weeks). Group 3 has higher new bone volume than that of Group 2 at 4, 8 and 12 weeks ($p < 0.05$) (Fig. 6).

Discussion

In the present study as well as our previous experiments, we have fabricated a 2D structure periosteum equvalent based on tissue-engineering principle, namely TEP. We proposed that this kind of flexible cellular loading construct may mimic a periosteal response during initiation of bone defect repair.

The TEP is fabricated by combining SIS with osteoblasts (induced from MSCs), which offers advantages over other tissues as graft material, since it is easy to handle and enhance vascularization [17, 18, 23]. Moreover, it produces low immune reaction [24].The thickness (100 ± 20 μm) of SIS is lower than the critical value (500 μm), can permit attached cells to survive on diffusion of nutrients from the interstitial fluid in early stage after implanting [25]. Successful bone formation was observed in Group1 and 3 via this TEP approach in this study.The findings suggested that TEP might regenerate bone tissue directly via survived cells attached on it.This hints that any size and any shape of bone defect can successfully repair via mimic peristeal approach without pre-vascularization of constructs, which is a critical challenge in tissure engineering area till now [26–27].

The histological inspection showed that the volume of newly formed bone in group1 was significantly higher than that in Group 2 and 3, and Group 3 was significantly higher than group 2 in the same period, which indicated that TEP had an osteogenic bioactivity. These findings were in accordance with our previous studies in long bone defect of rabbit models [17, 18].

In this study, the radiographic score in TEP-DPB hybrided implantation (Group 3) was higher than TEP or DPB grafting only.But that was inconsistent with histological findings. Decellularization protocols have to efficiently remove immunogenic materials, maintaining the nonimmunogenic ECM, which is endowed with specific inductive actions due to its architecture and bioactive factors [28]. As control scaffold in this study in Group 2 and 3, DPB from allogeneic scapula, which remains the 3D structure, porous microstructure and osteoinductive nature and was a relatively safe bone graft materials due to protein-free that might release immunorejection [29]. Meanwhile, DPB was degraded in vivo and substituted by new bone, but this osseointegration is a slow process called creeping substitution [14, 30]. It might be the

reason that new bone formation in Group 2 was slower than Group 1 and 3, and the radiological result was inconsistent with histological findings.

In Group 3, DPB combined with TEP, the former served as a shape guiding scaffold and mechanical support for TEP during new bone regenerating, while the latter was used as vital component endowed with osteogneic bioactivity.This hybrid was presumed that the new bone formation would be abundant via biomimetic periosteum, meanwhile, in accordance with the shape of DPB scaffold. The findings showed that the newly formed bone tissue in Group 3 was more than Group 2, but fewer than Group 1, though maintaining approximate shape of DPB scaffold. As we speculating, this might be the result from the DPB scaffold absorbed slower than new bone formation via TEP approach.

In Group 1, new bone formation was abundant, and formed approximate shape of scapular body, though it was in the absence of shape guiding 3D scaffold. The tensioned TEP attached to three anchoring points, as described above in surgical section, keep it maitaining triangular shape in Group 1, and that might provide the contour of irregular bone formation in almost shape of scapular body. Moreover, the new bone regenerate was more abundant than Group 3, which bone formation might be hindered by delayed degradation of DPB scaffold. As the literature reported, the remodeling of allograt bone occurs at a very slow rate and the necrotic bone cannot be completely replaced by new bone [31, 32]. This means that BTE made a balance between scaffold absorption and new bone formation may be important in future study and much more practical for widespread clinical use [23, 33].

Vascularity is essential for providing optimal blood supply to maintain survival of the osteogenic cells [34, 35]. In this study, 2D structure of TEP could permit attached cells to survive on diffusion of nutrients from the interstitial fluid in early stage [28].Moreover, SIS used as the scaffold of TEP in this study has strong angiogenic effects and retains plentiful bioactive components such as vascular endothelial growth factor (VEGF) [19, 36]. This advantage of SIS might contribute partially to vascularization during bone regenration in latter stage. In present study, TEP in vitro fabracation was simplified with only two components, SIS and MSCs, and we just used body as in vivo bioreactor to regenerate new bone as well as accompanied vessels, nerves and other affiliated tissues, according to the tissue engineering concept of some researchers [5, 33]. So, the in vivo osteogensis and aniogensis might be much more complicated beyond our speculation presently. It needs intensively study in the future.

The components of TEP, MSCs and SIS have great immune advantages and suitable for allografting [24]. Thus provides promise of off-the-shelf products in clinics in future application. Tissue-engineered bone via TEP approach in this study demonstrated an approximate shape of scapula.In the future, customized fabrication technique, such as three-dimensionally printing, with intelligent materials, whose degradation would be synchronized with new bone formation, would provide a precise repair for segmentally irrgelar bone defect via TEP approach [1, 4].

In this study, there are several limitations that need for further study. First, we have not tested the mechanism for bone formation of the TEP approach via intramembranous ossifcation or endochondral ossification in this study. Second, it may be necessary to use native periosteum as a control to compare

the effciency of bone formation of TEP approach in future experimentation. Third, it may be necessary to elaborate in vivo osteogensis and aniogensis in detail via TEP approach.

Conclusion

Massive irregular bone defect remains a challenge for orthopedic surgeons.In the present study, we have exploited a novel flexible periostem equivalent, namely TEP. The results obtained demonstrated that irregular bone defect could repair via TEP approach. It suggests that TEP has great potential for repair of massive irregular bone defect. Allogeneic DPB scaffold can provide mechanic support and shape guide for TEP osteogenesis, but hinder new bone formation due to retard absorption. Hopefully, customized and intelligent 3D scafffold, superior to DPB, would provide a more precise shape guiding in repair of irrgelar bone defect via TEP approch in future study.

The developed flexible TEP could represent an innovative approach to reconstruct any size and any shpe of massive bone defect via tissue engineering approach.

Abbreviations

TEP:Tissue-engineered periosteum; MSCs:Mesenchymal stem cells; SIS:Small intestinal submucosa; DPB:Deproteinized bone ; 3D:Threee-dimentional; BTE:Bone tissue engineering; CSD:critical size defect ; NZWRs:New Zealand white rabbits; DMEM:Dulbecco's modified Eagle medium; CO2:Carbon dioxide; Co-60:Cobalt-60; kGy:Kilogray; FBS:Fatal bovine serum; SEM:Scanning electron microscopy; H_2O_2:Hydrogen peroxide; NaN3:Sodium azide; NaOH:Sodium hydroxide; EDTA:Ethylene diamine tetraacetic acid; HE:Hematoxylin & eosin; ROI:Region of interest; M ± SD:Mean ± standard deviation; ANOVA:One-way analysis of variance; VEGF:Vascular endothelial growth factor.

Declarations

Ethics approval and consent to participate

All the experimental procedures involving animals were approved by the Institutional Animal Care and Use Committee of Lanzhou University, China.

Consent for publication

Not applicable.

Availability of data and material

Materials used and data collected in this study are available from the corresponding author on reasonable request.

Competing interests

The authors have no conflict of interest, financial or otherwise.

Funding

This work was finacially supported by the Featured Clinical Discipline Project of Shanghai Pudong (Pwzts2018-02) and the National Natural Science Foundation of China (30973064) .

Authors' contributions

Jiajia Yu and Cangyu Zhang performed the experiment, analyzed and interpreted the data, and Jiajia Yu drafted the manuscript. Lin Zhao participated in the design, coordination of the study, analysis and interpretation of data. He revised the manuscript and approved the final version to be submitted for publication. All authors read and approved the final manuscript.

Acknowledgements

Orthopaedic Institute of the 2nd Hospital of Lanzhou University (Lanzhou 730030, China) is acknowledged for the support of this work.

References

1. Zheng X, Huang J, Lin J, Yang D, Xu T, Chen D, Zan X, Wu A.3D bioprinting in orthopedics translational research. J Biomater Sci Polym Ed. 2019;30:1172-87.
2. Jiang H, Cheng P, Li D, Li J, Wang J, Gao Y, Zhang S, Cao T, Wang C, Yang L, Pei G. Novel standardized massive bone defect model in rats employing an internal eight-hole stainless steel plate for bone tissue engineering. J Tissue Eng Regen Med. 2018;12:e2162-71.
3. Shanbhag S,Pandis N,Mustafa K,Nyengaard JR,Stavropoulos A.Cell Cotransplantation Strategies for Vascularized Craniofacial Bone Tissue Engineering: A Systematic Review and Meta-Analysis of Preclinical In Vivo Studies. Tissue Eng Part B Rev. 2017;23:101-7.
4. Huang YH, Jakus AE, Jordan SW, Dumanian Z, Parker K, Zhao L, Patel PK, Shah RN.Three-Dimensionally Printed Hyperelastic Bone Scaffolds Accelerate Bone Regeneration in Critical-Size Calvarial Bone Defects. Plast Reconstr Surg. 2019;143:1397-407.
5. Huang RL,Liu K,Li Q.Bone regeneration following the in vivo bioreactor principle: is in vitro manipulation of exogenous elements still needed?. Regen Med.2016;11:475-81.
6. Landman KA, Cai AQ.Cell proliferation and oxygen diffusion in a vascularising scaffold. Bull Math Biol.2007;69:2405-28.
7. Santos MI, Reis RL.Vascularization in bone tissue engineering: physiology, current strategies, major hurdles and future challenges. Macromol Biosci. 2010;10:12-27.
8. Yu H, VandeVord PJ, Mao L, Matthew HW, Wooley PH, Yang SY. Improved tissue-engineered bone regeneration by endothelial cell mediated vascularization. Biomaterials.2009;30:508-17.

9. Lin CY, Chang YH, Lin KJ, Yen TC, Tai CL, Chen CY, Lo WH, Hsiao IT, Hu The healing of critical-sized femoral segmental bone defects in rabbits using baculovirus-engineered mesenchymal stem cells. Biomaterials.2010;31:3222-30.
10. Fidkowski C, Kaazempur-Mofrad MR, Borenstein J, Vacanti JP, Langer R, Wang Y.Endothelialized microvasculature based on a biodegradable elastomer. Tissue Eng. 2005;11:302-9.
11. Percival CJ, Richtsmeier JT. Angiogenesis and intramembranous osteogenesis. Dev Dyn. 2013;242: 909–22.
12. Orwoll ES. Toward an expanded understanding of the role of the periosteum in skeletal health. J Bone Miner Res. 2003;18:949–54.
13. Wlodarski KH. Normal and heterotopic periosteum. Clin Orthop Relat Res. 1989; 241:265–77.
14. Zhang X, Awad HA, O'Keefe RJ, Guldberg RE, Schwarz EM. A perspective: engineering periosteum for structural bone graft healing. Clin Orthop Relat Res. 2008;466:1777–87.
15. Ouyang HW, Cao T, Zou XH et al. Mesenchymal stem cell sheets revitalize nonviable dense grafts: implications for repair of large-bone and tendon defects. Transplantation. 2006;82:170–4.
16. Knothe Tate ML, Ritzman TF, Schneider E, Knothe UR. Testing of a new one-stage one-transport surgical procedure exploiting the periosteum for the repair of long-bone defects. J Bone Joint Surg Am. 2007;89:307–16.
17. Lin Zhao, Junli Zhao, Jiajia Yu, Rui Sun , Xiaofeng Zhang , Shuhua Hu.In vivo investigation of tissue-engineered periosteum for the repair of allogeneic critical size bone defects in rabbits. Regen Med. 2017;12:353-64.
18. Lin Zhao, Junli Zhao, Jiajia Yu, Xiaofei Zhao, QiChen, Yanfeng Huang. In vitro study of bioactivity of homemade tissue-engineered periosteum. Mater Sci Eng C Mater Biol Appl. 2016;58:1170-6.
19. Luo JC, Chen W, Chen XH, Qin TW, Huang YC, Xie HQ, Li XQ, Qian ZY, Yang A multi-step method for preparation of porcine small intestinal submucosa (SIS). Biomaterials. 2011;32:706-13.
20. Zhao M, Zhou J, Li X, Fang T, Dai W, Yin W, Dong J. Repair of bone defect with vascularized tissue engineered bone graft seeded with mesenchymal stem cells in rabbits. Microsurgery. 2011;31:130-7.
21. Lane JM, Sandhu HS. Current approaches to experimental bone grafting. Orthop Clin North Am. 1987;18:213–25.
22. Rodrigues MT, Gomes ME, Reis RL. Current strategies for osteochondral regeneration: from stem cells to pre-clinical approaches. Curr Opin Biotechnol. 2011;22:726-33.
23. Cancedda R, Giannoni P, Mastrogiacomo M. A tissue engineering approach to bone repair in large animal models and in clinical practice. Biomaterials. 2007;28: 4240-50.
24. Lin Zhao, Junli Zhao, Shuanke Wang, Yayi Xia, Jia Liu , Jin He, Xin Wang. Evaluation of immunocompatibility of tissue-engineered periosteum. Biomed Mater. 2011; 6:015005.
25. Ye H, Xia Z, Ferguson DJ, Triffitt JT, Cui Z. Studies on the use of hollow fibre membrane bioreactors for tissue generation by using rat bone marrow fibroblastic cells and a composite scaffold. J Mater Sci Mater Med .2007;18:641-8.

26. Sasaki JI, Katata C, Abe GL, Matsumoto T, Imazato S. Fabricating large-scale three-dimensional constructs with living cells by processing with syringe needles.J Biomed Mater Res A. 2019;107:904-9.
27. Mi HY, Jiang Y, Jing X, Enriquez E, Li H, Li Q, Turng LS. Fabrication of triple-layered vascular grafts composed of silk fibers, polyacrylamide hydrogel, and polyurethane nanofibers with biomimetic mechanical properties. Mater Sci Eng C Mater Biol Appl. 2019;98:241-9.
28. Porzionato A, Stocco E, Barbon S, Grandi F, Macchi V, De Caro R. Tissue-Engineered Grafts from Human Decellularized Extracellular Matrices: A Systematic Review and Future Perspectives. Int J Mol Sci .2018;19: pii: E4117.
29. Zhou Y, Guan X, Wang H, Zhu Z, Li C, Wu S, Yu H. Hypoxia induces osteogenic/angiogenic responses of bone marrow-derived mesenchymal stromal cells seeded on bone-derived scaffolds via ERK1/2 and p38 pathways.Biotechnol Bioeng. 2013;110:1794-804.
30. Cobos JA, Lindsey RW, Gugala Z. The cylindrical titanium mesh cage for treatment of a long bone segmental defect: description of a new technique and report of two cases. J Orthop Trauma. 2000;14:54-59.
31. Burchardt H. Biology of bone transplantation. Orthop Clin North Am. 1987;18:187–96.
32. Bauer TW, Muschler GF. Bone graft materials. An overview of the basic science. Clin Orthop Relat Res. 2000;371:10–27.
33. Service RF.Tissue engineering. Technique uses body as 'bioreactor' to grow new bone. Science. 2005;309:683.
34. Leunig M, Demhartner TJ, Sckell A, Fraitzl CR, Gries N, Schenk RK, Ganz R. Quantitative assessment of angiogenesis and osteogenesis after transplantation of bone: comparison of isograft and allograft bone in mice. Acta Orthop Scand. 1999;70:374–80.
35. Leunig M, Yuan F, Berk DA, Gerweck LE, Jain RK. Angiogenesis and growth of isografted bone: quantitative in vivo assay in nude mice. Lab Invest 1994;71:300–7.
36. Sun T, Liu M, Yao S, Ji Y, Xiong Z, Tang K, Chen K, Yang H, Guo X. Biomimetic Composite Scaffold Containing Small Intestinal Submucosa and Mesoporous Bioactive Glass Exhibits High Osteogenic and Angiogenic Capacity. Tissue Eng Part A. 2018;24:1044-56.

Figures

Figure 1

Schematic drawing of surgery. The segmentally irregular bone defect model and shaped implants repair.

Figure 2

Seeding cells and implants, (a) the primary passage of MSCs, (b) the 3rd passage of MSCs with HE staining, (c) Alizarin red staining determined calcified colliculus formation from osteogenically induced MSCs, (d) Appearance of SIS under SEM,(e) cells attached on TEP under HE staining inspection,(f) cells attached on TEP under SEM inspection,(g) Macroscopical appearance of SIS,(h)Macropscopical appearance of DPB implants,(i) Macroscopical appearance of TEP in culture dish.

Figure 3

X-ray radiograph and macroscopic observation.The 1st row (a,b and c) represents X-ray radiograph of scapular defect repair in Group1 at 4, 8 and 12 weeks respectively. The 2nd row (d,e and f) represents X-ray radiograph of scapular defect repair in Group2 at 4, 8 and 12 weeks respectively. The 3rd row (a,b and c) represents X-ray radiograph of scapular defect repair in Group3 at 4, 8 and 12 weeks respectively.The 4th column (j,k and l) represents macroscopical view of scapular defect repair in Group1,2 and 3 at 12 weeks respectively.

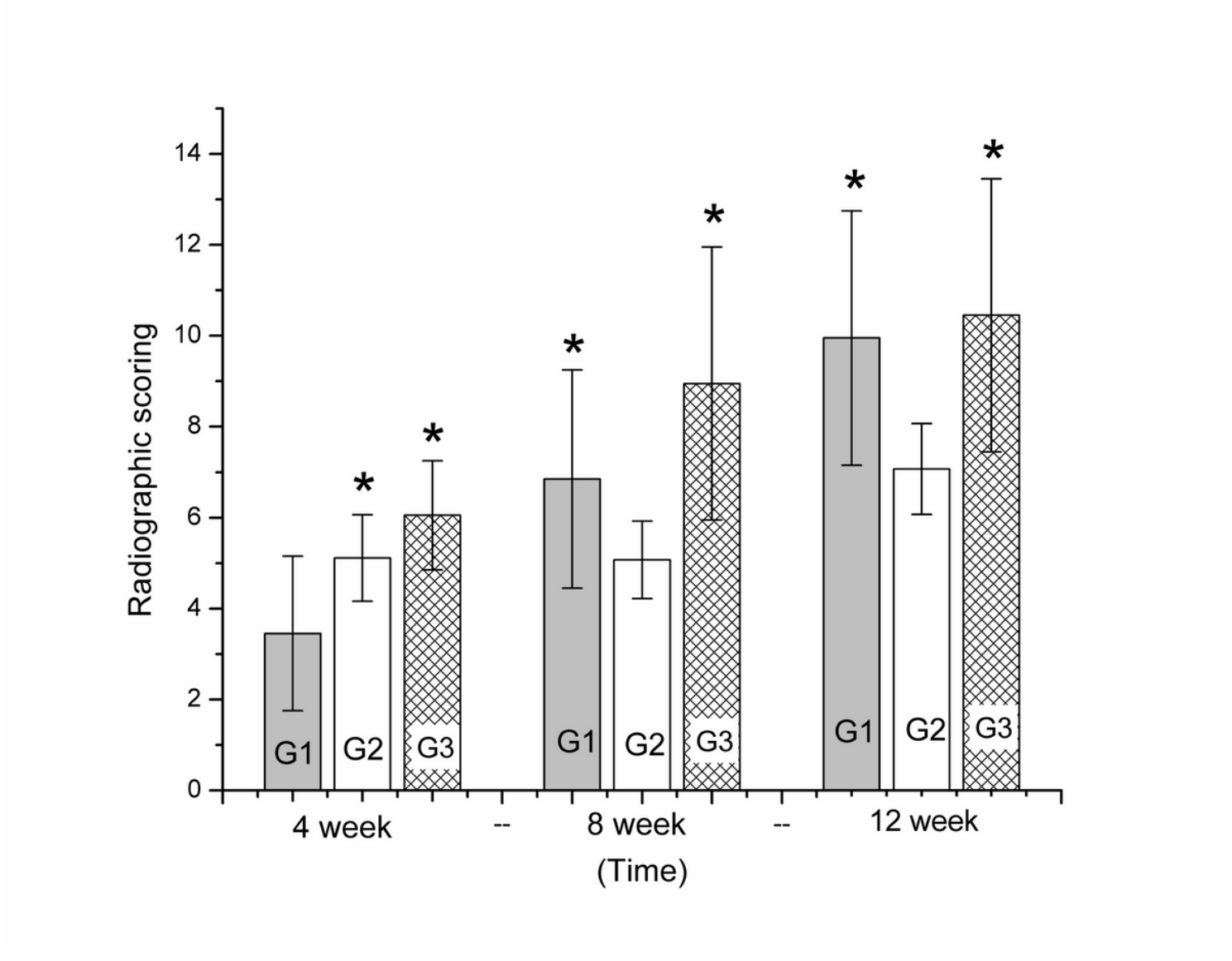

Figure 4

Histogram of radiographic scores of each groups at 4, 8 and 12 weeks. “*” represents signifcant difference between different groups at the same time.G1,2 and 3 respectively represenrs Group1,2 and 3.

Figure 5

Histological examination with HE (row 1,3 and5) and Masson (row 2,4 and 6) staining. In Group1(row1,2), TEP formed island-like calluses at 4 weeks (a,b). New bone tissue increased with irregular vessels or immature marrow cavities, while TEP disappeared off (possibly degraded) at 8 weeks (c,d). At 12 weeks, all newly formed bone developed into mature cancellous bone (e,f). In Group2 (row3, 4), DPB was mainly surrounded by scar tissue and infiltrated lymphocytes at 4 weeks (g,h), and accompanied with few new osseous tissue formation at 8 (i,j) and 12 weeks(k,l). In Group3 (row5, 6), there was a few of new bone formation between TEP and DPB, which were degraded accompanied by scar tissue at 4 weeks (m,n).New osseous tissue formed woven bone at 8 weeks(o,p), while it was inclinded to form mature lamellar bone with osteoblasts embeded into mineral matrix at 12 weeks(q,r). Triangles represent TEP, black arrows represent newly formed bone tissue, white arrows represent remnants of DPB. Bars = 1mm.

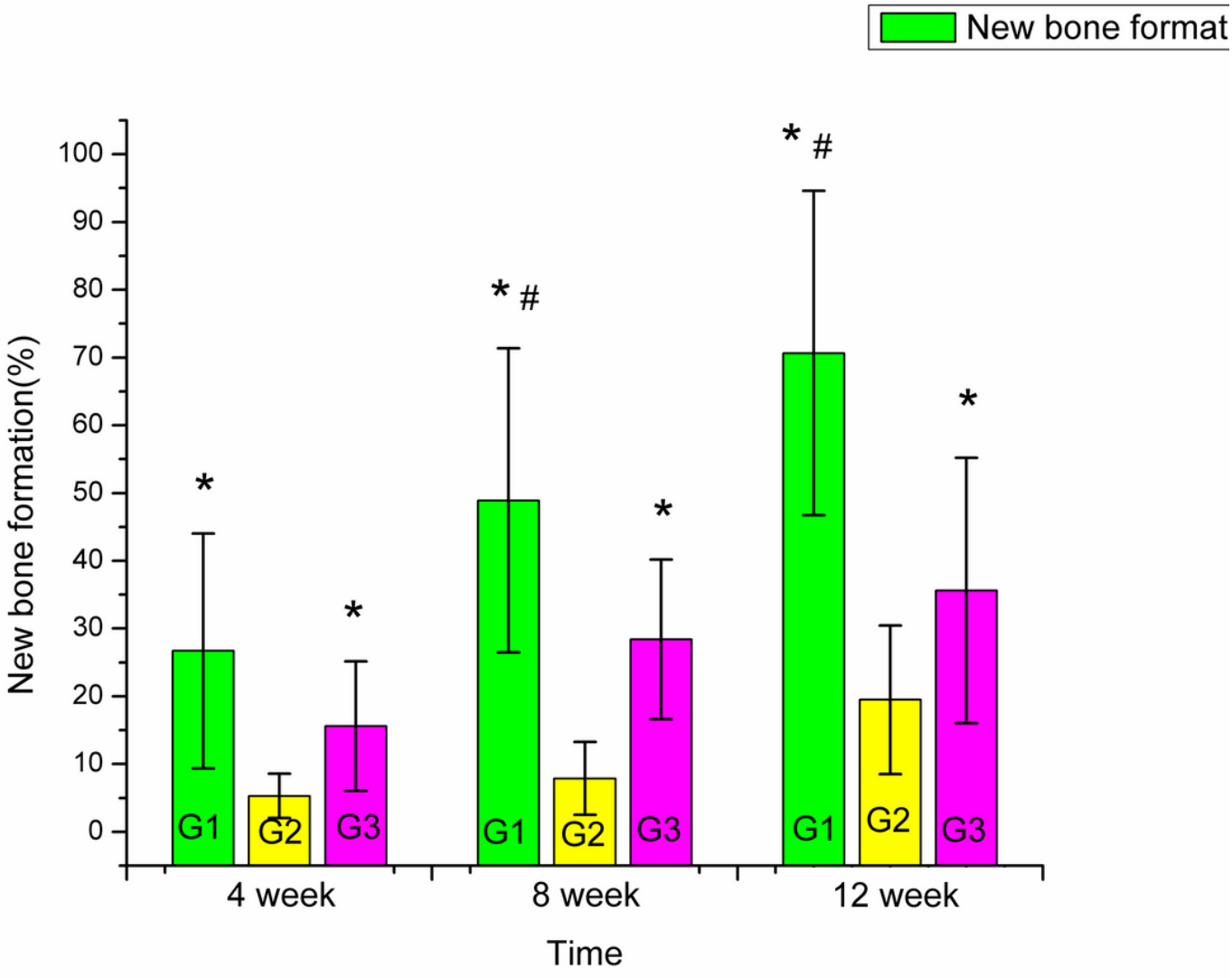

Figure 6

Histogram of histological scores of each groups at 4, 8 and 12 weeks. “*” and “*#”represent signifcant difference between different groups at the same time (*p < 0.05 and *#p < 0.001).G1,2and 3 respectively represenrs Group1,2 and 3.

Supplementary Files

This is a list of supplementary files associated with this preprint. Click to download.

- NC3RsARRIVEGuidelinesChecklist01.pdf